Anisotropy of the probability of electron scattering by phonons on the Fermi surface of copper

V. F. Gantmakher and V. A. Gasparov
Institute of the Physics of Solids, USSR Academy of Science
(Submitted December 2, 1972)
Zh. Eksp. Teor. Fiz. **64**, 1712-1723 (May 1973)

The electron-phonon collision frequencies, averaged over the extremal orbits, are obtained for 20 orbits in copper from measurements of the temperature dependences of the radio-frequency size-effect line amplitudes. The collision frequency as a function of the point on the Fermi surface is determined by mathematical treatment of the data. The results are represented on a stereographic projection. The relation between the collision frequency measured experimentally and the electron-phonon interaction matrix element is analyzed.

This research is devoted to the experimental investigation of the dependence of the electron-phonon collision frequency in copper on the position of the electron on the Fermi surface. As initial data, we used the temperature dependences of the line amplitudes of the radio-frequency size effect on the closed trajectories for various directions of the magnetic field.

As is known, the size-effect lines are produced by a comparatively narrow layer of orbits on the Fermi surface, located near the extremal orbit, and the line amplitude is proportional to the number of electrons from this layer which pass without scattering from one side of the plate to the other. Therefore, the temperature dependence of each separate line gives electron-scattering information averaged over the points lying along the corresponding extremal orbit on the Fermi surface. If the network of the investigated orbits covers the entire Fermi surface sufficiently densely, then a suitable mathematic procedure allows us to find the scattering probability as a function of the point on the surface.[4]

Copper is one of the few metals for which this program can be carried out at the present time, since the mathematical treatment of the experimental results makes it necessary to specify the Fermi surface $\Psi(\mathbf{k}) = 0$ of the metal in k space and the velocity $\mathbf{v}(\mathbf{k})$ distribution on it with sufficiently great accuracy. We have used in our calculations the parameters of the electron spectrum of copper which are given in the work of Halse.[2]

The frequency of the electron-phonon collisions in copper for a whole series of points on the Fermi surface was recently measured by Doezema and Koch[3] by using the temperature dependence of the line shapes of the resonances on the magnetic surface levels. The agreement of our and their results serve as a confirmation of the correctness of both methods, which is important, since the two methods were in fact used for the first time in a detailed study of the anisotropy of electron-phonon scattering.

THEORETICAL BASES OF THE METHOD

The amplitude of the size-effect lines on closed trajectories is

$$A(T) \sim [\exp(\pi\bar{\nu}_{\text{eff}}/\Omega) - 1]^{-1}, \tag{1}$$

where $\Omega = eH/mc$ is the cyclotron frequency (H is the magnetic field, e and m the charge and cyclotron mass of the electron), and the effective collision frequency is the sum of the effective frequencies $\bar{\nu}_0$ of the collisions with impurities and other static defects and $\bar{\nu}(T)$ with phonons: $\bar{\nu}_{\text{eff}} = \bar{\nu}_0 + \bar{\nu}(T)$. In principle, the frequency of electron-electron collisions also enters in $\bar{\nu}(T)$; however, from the temperature dependence of $\bar{\nu}(T)$ in copper, measured by different methods in a number of researches[3-5] ($\bar{\nu} \sim T^3$), it follows that collisions with phonons predominate in $\bar{\nu}$ for copper. If $\pi\bar{\nu}_{\text{eff}}/\Omega \gg 1$, so that the electron can make only a half revolution along its trajectory in the entire range of temperature studied, then Eq. (1) is materially simplified:

$$A(T) \sim \exp(-\pi\bar{\nu}/\Omega) \tag{2}$$

and becomes very convenient for the measurement of $\bar{\nu}(T)$.

The fact that the argument of the exponential in (1) and (2) is expressed not in terms of the path length, as is customary, but in terms of ν, is important in two ways. First, the scattering probability has a more explicit physical meaning and it is more naturally compared with theory. Second (and this is the more important), when this form is used, it is not necessary in the treatment of the results, to calculate the path length of the electron from one side of the plate to the other along the trajectory, but one can use the known values of the cyclotron masses. It is then more natural to use for H in the expression for Ω not the cutoff field, which corresponds to the left edge of the line, but the value of the field in that part of the line where the amplitude A is measured, i.e., the half-way between the characteristic extrema of the line.

The main experimental result that must be compared with theory is the frequency of the electron-phonon collisions as a function of the point on the Fermi surface. We shall first analyze its connection with the parameters of electron-phonon interaction and with the quantity $\bar{\nu}$, measured in the experiments. The amplitude of the size-effect line reflects the change due to the collisions of the nonequilibrium increment Δf of the electron distribution function. We choose a phonon with such a wave vector q and energy ϵ that the collisions with it are allowed by the conservation laws. The changes Δf at the point k are due both to the change in the number of departures from the state k in collisions with the phonon q:

$$\Delta N_{\text{dep}} \sim \Delta f[\varphi_\varepsilon(1 - f_{E+\varepsilon}) + (\varphi_\varepsilon + 1)(1 - f_{E-\varepsilon})], \tag{3}$$

and to the change, as a consequence of the Pauli princi-

ple, in the number of arrivals into the state $\mathbf{k}$ from the state $\mathbf{k} \pm \mathbf{q}$:

$$\Delta N_{\text{arr}} \sim -\Delta f[\varphi_\varepsilon f_{E-\varepsilon} + (\varphi_\varepsilon + 1) f_{E+\varepsilon}] \tag{4}$$

(here E is the initial energy of the electron, f_E and φ_ϵ are the distribution functions of the electrons and phonons; the two components in square brackets in (3) and (4) reflect the presence of two types of collisions: with absorption and with emission of phonons).

The total change in the number of particles, normalized to a single electron, is equal to[6]

$$-\frac{\Delta N}{\Delta f} = \frac{1}{\Delta f}(\Delta N_{\text{dep}} - \Delta N_{\text{arr}}) \sim 2\varphi_\varepsilon + 1 + f_{E+\varepsilon} - f_{E-\varepsilon} \equiv \Phi(E, \varepsilon).$$

Inasmuch as the nonequilibrium increments to the functions φ_ϵ and f_E are small, we have

$$\Phi(E, \varepsilon) = \frac{(e^\alpha + 1)^2 (e^\beta + 1)}{(e^\beta - 1)(e^{\alpha+\beta} + 1)(e^{\alpha-\beta} + 1)}, \quad \alpha = \frac{E - E_F}{k_B T}, \quad \beta = \frac{\hbar q s}{k_B T} \tag{5}$$

(E_F is the Fermi energy, k_B the Boltzmann constant). The total frequency of collisions with phonons is

$$\nu = \frac{1}{2\pi^2 \hbar} \int M^2(\mathbf{k}, \mathbf{q}) \Phi(E\ \varepsilon) \delta(E_{\mathbf{k}'} - E_{\mathbf{k}} - \varepsilon) d^3q, \tag{6}$$

where $\mathbf{k}' = \mathbf{k} \pm \mathbf{q}$, the δ function guarantees the satisfaction of the conservation laws, and M^2 is the square of the interaction matrix element. In the simplest model[7]

$$M^2(\mathbf{k}, \mathbf{q}) = \hbar q \Delta^2 / 2\mu s \tag{7}$$

(Δ is the deformation-potential constant, s the speed of sound, μ the mass of a unit volume of the crystal).

The expression (6) depends on the energy of the initial state of the electron. In such kinetic effects as the size effect, the increment Δf is proportional to $\partial f_E^{(0)}/\partial E$, where $f_E^{(0)}$ is the equilibrium distribution function. This means that the nonequilibrium electrons of interest to us all have an energy within the limits of the thermal spread. In this interval, ν changes little in comparison with its mean value, which allows us, by averaging the quantity ν itself along the normal to the Fermi surface:

$$\nu^*(k_F) = \int_0^\infty \nu(E) \Delta f\, dE \Big/ \int_0^\infty \Delta f\, dE, \tag{8}$$

To use the value ν^* already averaged over the energy in the final expression for the line amplitude.

Substituting Eqs. (5)—(7) in (8), and changing the order of integration, we obtain (under the assumption that the radius of curvature of the Fermi surface $k_F \gg k_B T/\hbar s$, cf.[8])

$$\nu^*(k_F) = \frac{1}{2\pi} \frac{\Delta^2 (k_B T)^3}{\hbar^4 s^4 \mu v} \int_0^\infty \frac{x^3 e^x dx}{(e^x - 1)^2} = \frac{3\zeta(3)}{\pi} \frac{\Delta^2 (k_B T)^3}{\hbar^4 s^4 \mu v}, \tag{9}$$

where the ζ function $\zeta(3) = 1.20$, and v is the Fermi velocity. The subscript index F in the argument of the function ν^* in (9) serves to emphasize the fact that now the argument takes on only values lying on the Fermi surface itself, since the averaging takes place along the normal to it.

Actually, the deformation potential is a tensor $\tilde{\Delta}$ and enters in the matrix element in the form of the combination

$$\Delta_{ij} \partial u_i / \partial x_j \sim (\mathbf{e}\tilde{\Delta}\mathbf{q}),$$

where $\mathbf{u}$ is the deformation vector, and $\mathbf{e}$ is the unit vector of the phonon polarization. Replacing $\tilde{\Delta}$ by a scalar and taking some average value s, we discard from $M^2(\mathbf{k}, \mathbf{q})$ factors of the type of the square of the cosine between $\mathbf{e}$ and $\tilde{\Delta}\mathbf{q}$; on the other hand, we integrate in (6) along one of the acoustic branches, in correspondence with the fact that, for a scalar Δ, $M^2 = 0$ for phonons with a purely transverse polarization. Therefore, the final result of the experiment, which is subject to comparison with theory, must be taken to be the collision frequency $\nu^*(\mathbf{k}_F)$ and not the scalar function $\Delta(\mathbf{k}_F)$ connected with it by Eq. (9). The meaning of the numerical coefficient in (9) is that it emphasizes that in calculations of $\nu^*(\mathbf{k}_F)$ it is necessary to use the function $\Phi(\mathbf{E}, \epsilon)$ in the form (5) and to average (8) over the energy.

In order to establish a connection between $\nu^*(\mathbf{k}_F)$ and the quantity $\tilde{\nu}$ which enters in Eqs. (1) and (2), it is necessary to average ν^* over states along the extremal orbit. Here, however, complications can arise, associated with the effectiveness of the electron-phonon collisions in the size effect. When scattered by a thermal acoustic phonon, an electron is displaced along the Fermi surface by a distance $q_T \approx k_B T/\hbar s$. This change in the wave vector of the electron is reflected in the line amplitude A, only in the case when q_T is larger than the dimensions of the range of effectiveness on the Fermi surface, i.e., the region in which $\Delta f \neq 0$. For the size effect on closed trajectories, the dimensions of the region vary along the extremal orbit: they are of the order $(\delta/d)k_F$ (δ is the depth of the skin layer, d the thickness of the plate) wherever the electron moves along the normal to the surface of the plate, and of the order $(\delta/d)^{1/2}k_F$ where it moves along the surface itself.[9]

If $q_T/k_F > (\delta/d)^{1/2}$, then any collision with a phonon makes the electron ineffective. Then

$$\bar{\nu}_j = \frac{\hbar}{2\pi m_j} \oint_j \frac{\nu^* dk}{v_\perp} \tag{10}$$

($v_\perp$ is the projection of the velocity of the electron on the plane of the orbit and the index j denotes the set of data specifying the extremal orbit). In our experiments, however, the inequality

$$(\delta/d)^{1/2} > q_T/k_F > \delta/d \tag{11}$$

holds, so that the effectiveness of the collisions can change along the trajectory. In order to take this circumstance into account, we have assumed, in purely model fashion, that averaging in (10) gives rise to an additional weighting factor

$$\bar{\nu}_j = \frac{\hbar}{2\pi m_j} \oint_j \frac{\nu^* |\cos\gamma| dk}{v_\perp}, \tag{12}$$

where γ is the angle between the electron velocity $\mathbf{v}$ and the normal to the surface of the sample.

Thus, in experiments on the size effect, one can measure the quantity $\tilde{\nu}$ for various orbits; Eq. (12) (or (10)) allows us in principle to find the function $\nu^*(\mathbf{k}_F)$ from them, making possible a comparison with theory.

EXPERIMENT

The amplitudes of the size-effect lines were measured on plots of the derivatives of the magnetic field with respect to the real part of the surface impedance, $\partial R/\partial H$ or $\partial^2 R/\partial H^2$, in the frequency range 1—8 MHz (the modulation frequency of the magnetic field was

18 Hz). An autodyne generator was connected in a negative feedback loop of the type proposed by Egorov.[10] This allowed us to carry out studies over a wide temperature interval at a practically constant sensitivity of the recording circuit. Furthermore, the stabilization of the amplitude of oscillations made it possible to operate at low levels of generation ($\lesssim 0.1$V), which guaranteed the absence of heating of the sample (relative to the thermometer) by the induction currents.

Measurements were carried out over the temperature range 1.5–12°K. The coil of the generator, together with the sample inserted in it, was located inside a copper vacuum-tight vessel filled with gaseous helium. The temperature was regulated by means of a bifilarly wound heater wire on the outer surface of the vessel. Thermal isolation of the vessel from the tank with liquid helium was accomplished by the use of a foam plastic covering, sealed with vacuum grease that hardened upon cooling. The temperature was determined by measuring the resistance of a 100-ohm Allen-Bradley radio resistor with a power rating of 0.1 W. The thermometer was calibrated against the vapor pressure of liquid helium in the range 1.5–4.2°K and against the superconducting transition for lead; in the region of higher temperature, the calibration was extrapolated according to the formula

$$T^{-1} = \sum_{n=0}^{3} a_n (\lg r)^n.$$

The accuracy achieved, which we estimate at $\pm 0.02°$, appreciably exceeded that necessary for reduction of the measurements.

Samples in the shape of plane parallel plates were cut from single-crystal bars. Five samples were used with the normal to the surface of the plate along the [100] axis, and eight samples with the normal along [110] (the angle between the corresponding axis and the normal did not exceed 1°). The first group of samples was prepared from copper which has a resistance ratio $r_{293°K}/r_{4.2°K}$ of about 400 before annealing in oxygen and 7000 after annealing; the second was prepared from purer copper[1)] with a resistance ratio of 7000 and 14000. The method of preparation of the samples has been described in detail in a previous paper.[11] Most of the measurements were carried out on samples of thickness 0.5–0.8 mm (the relative line widths here were 3–4%). The measurements of amplitude of the neck size-effect lines were made on very thin samples of 0.2–0.35 mm (line widths about 8%).

For amplitude measurements, it is important that the shape and width of the lines do not change throughout the entire temperature range. At the same time, it is known that under conditions when the electron returns many times to the skin layer, the skin-layer thickness δ and the width of the size-effect line depend on the path length l.[12] All our measurements were made in a field H parallel to the surface of the sample, so that multiple reentries of electrons in the skin layer were possible in principle. Therefore, we checked the constancy of the shape and of the width of the lines in each series of measurements. Changes actually took place for the size-effect line from the central sections in thin (0.2–0.3 mm) samples. There were no changes in thick samples which, in addition to everything else, indicates the absence of multiple reentries and the applicability of Eq. (2). For the neck size-effect lines, samples of thickness 0.2–0.3 mm were thick enough.

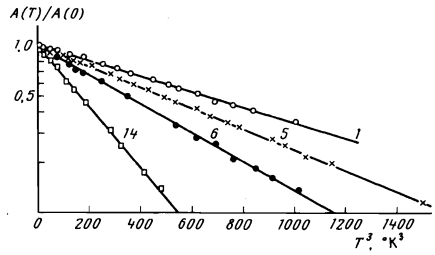

FIG. 1. Temperature dependences of the amplitude of the size effect lines on a sample of copper of thickness d = 0.53 mm with normal along the [100] axis. The frequency $\omega/2\pi = 3.5$ MHz. The numbers at the straight lines indicate the orbits in correspondence with the enumeration given in the table and in Fig. 2.

No. of orbit	$\varphi^* = 0$ θ*, deg	Origin of orbit	m/m_0	$\bar{\nu}/T^3 \cdot 10^{-6}$, $sec^{-1} \cdot °K^{-3}$	No. of orbit	$\varphi^* = 45°$ θ*, deg	Origin of orbit	m/m_0	$\bar{\nu}/T^3 \cdot 10^{-6}$, $sec^{-1} \cdot °K^{-3}$
1**	0	Central cross section	1.370	3.13	7**	0	Central cross section	1.370	3.10
2	5		1.365	3.10	8	8		1.365	3.11
3	10		1.353	3.34	9	16		1.355	3.22
4	15		1.351	3.46	10	50		1.402	2.16
5	20		1.365	3.61	11	55		1.385	2.02
6	25		1.410	4.65	12	60		1.400	2.57
					13	65		1.458	3.48
14***	45		1.290	7.04	—	50	Neck	0.467	16.8
					15	55		0.46	22.4
					—	60		0.468	18.2
					—	65		0.500	17.8
					—	70		0.547	16.7
					****	55		1	1.17

*θ and φ are the spherical coordinates of the direction of the magnetic field ($\theta = 0$ corresponds to H ∥ [001], $\theta = 90°$, $\varphi = 0$ – H ∥ [100].

**Orbits 1 and 7 are distinguished by points of tangency of the trajectory with the surface of the sample.

***Orbit 14 is known in the literature under the name "dog bone."

****An open orbit, the effective mass for which is unknown; in the calculation of $\bar{\nu}/T^3$, we have tentatively set $m = m_0$.

The anisotropy of the orbits with extremal dimensions in copper were studied in detail by the size effect[13] and also by magnetoacoustic oscillations.[14] We used the results of these researches to identify the observed lines.

Inasmuch as the temperature range in which the measurements were carried out was always sufficiently large (see, for example, Fig. 1), the determination of the power of T in the function $\bar{\nu}(T)$ did not entail any difficulty. On all the orbits studied by us, the quantity $\bar{\nu}$ was undoubtedly proportional to T^3. The results of the measurement of the coefficient of proportionality as a function of the position of the orbit on the Fermi surface are shown in the table and in Fig. 2. The cyclotron masses in the (110) plane were taken from the work of Koch et al.,[15] and in the (100) plane from our calculations (see below).

The results were averaged over a large number of values obtained with various samples and in various experiments. The scatter of the points about the mean value did not exceed 10%, which characterizes the accuracy of our measurements.

According to Kamm's identification of the orbits[14], one of the lines measured by us (group 8 in the (100) plane in the Kamm notation) belongs to an open orbit. Therefore a conditional value of $\bar{\nu}$ is given in the table, computed under the assumption that the cyclotron mass

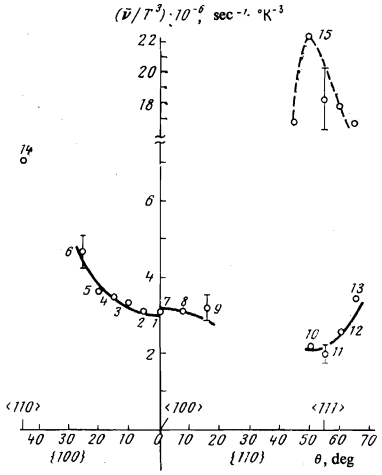

FIG. 2. Dependence of the collision frequency, averaged over the orbit, on the direction of the magnetic field. For convenience in the following discussion, the orbits were renumbered (see the table). The dashed line connects points obtained for orbits on the neck for various directions of **H**. See the text concerning the continuous lines near points 1-13.

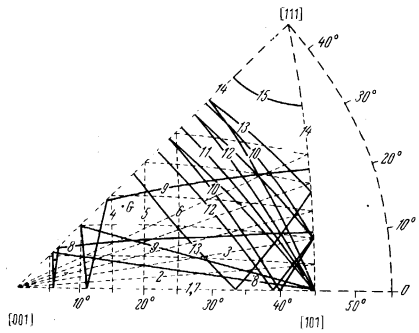

FIG. 3. Location of the studied orbits on the stereographic projection of the Fermi surface. The broken lines indicate orbits obtained for **H** in the {100} plane, the continuous lines – for **H** {110}. The orbits 1 and 7 are identical.

is equal to the mass of the free electron m_0. This point was not plotted in Fig. 2.

Because of the cubic symmetry, all the physically different points of the Fermi surface of copper can be mapped on 1/48 of the stereographic surface of a sphere (the vicinity of the [111] direction is occupied by the neck). Then each orbit has the shape of a broken line. As is seen from Fig. 3, the orbits studied by us form a sufficiently dense net covering the entire Fermi surface, with the exception of the immediate vicinity of the neck.

MATHEMATICAL TREATMENT OF THE RESULTS

In order to transform the values obtained for $\bar{\nu}_j$, i.e., to find the function $\nu^*(\mathbf{k})$ from them, we used the following procedure.[1] Representing $\nu^*(\mathbf{k})$ in the form of a sum of test functions:

$$\nu^*(\mathbf{k}) = T^3 \sum_{i=1}^{t} w_i F_i(\mathbf{k}), \tag{13}$$

substituting this sum in (12), and calculating the integrals over the sections of the surface $\Psi(\mathbf{k}) = 0$ by means of a computer:

$$a_{ij} = \frac{\hbar}{2\pi m_j} \oint_j \frac{F_i(\mathbf{k})\,|\cos\gamma|\,dk}{v_\perp(\mathbf{k})} = \frac{\hbar}{2\pi m_j} \int_0^{2\pi} \frac{k^2 F_i |\cos\gamma|\,|\nabla\Psi|\,d\xi}{(\mathbf{k}\nabla\Psi)\,|v|}, \tag{14}$$

we reduce Eqs. (12) to a set of algebraic equations:

$$\bar{\nu}_j/T^3 = \sum_i a_{ij} w_i, \quad j = 1, 2, \ldots, p; \quad i = 1, 2, \ldots, t, \tag{15}$$

in which the number of equations p is equal to the number of experimental points used, and the number t of the unknowns is equal to the number of terms in the sum (13). Naturally, the functions F_i should have cubic symmetry, as does the desired function $\nu^*(\mathbf{k})$, and the inequality $t < p$ should hold, inasmuch as the computed coefficients a_{ij} and (especially) the experimental values $\bar{\nu}_j$ are known only with a certain accuracy. The solution of the overdetermined set (15) is found from the condition of the minimum of the quadratic form:

$$\sum_{j=1}^{p} \frac{1}{\bar{\nu}_j^2} \left(\bar{\nu}_j - T^3 \sum_{i=1}^{t} a_{ij} w_i \right)^2 .$$

When choosing the set of test functions, we must keep the following in mind. Even for accurately known $\bar{\nu}_j$ and a_{ij}, the problem has an infinite number of solutions. Actually, the function $\nu^*(\mathbf{k})$, which is a solution of the problem, can be measured arbitrarily at those parts of the Fermi surface through which our p contours do not pass (for example, in the vicinity of the point G in Fig. 3), without spoiling Eqs. (12) here. It is natural that we must strive to find the simplest, smoothest solution from among all those which satisfy the experimental data. Therefore the test functions should oscillate as little as possible and their number should be as small as possible.

This same limitation follows from other considerations. Let us assume that the a_{ij} are calculated with relative accuracy $\eta = \Delta a_{ij}/a_{ij}$. Then we must have, for all j,

$$\frac{\Delta\bar{\nu}_j}{T^3} = \eta \sum_{i=1}^{t} |a_i w_i| \ll \frac{\bar{\nu}_j}{T^3}. \tag{16}$$

For each specific system of t test functions F_i, the inequality (16) means that the root (15) should not be so large in absolute value to make $\bar{\nu}_j$ in (15) a small difference between large numbers.

From the theoretical calculations of Nowak,[16] from the data of Doezema and Koch[3], and also from the preliminary analysis of our data, it follows that the desired function $\nu^*(\mathbf{k})$ has a very sharp maximum in the vicinity of the neck. In order not to increase the number of terms of the expansion (13), we have chosen to eliminate orbits 14 and 15, which pass through the neck, not to consider the function $\nu^*(\mathbf{k})$ obtained from (13) in the immediate vicinity of the neck, and to use the directly measured value $\bar{\nu}_{15}$ for ν^* on the neck (see the table).

As the test functions F_i we used the first terms of the Fourier series

$$F_{lnm}(\mathbf{k}) = \sum \cos\frac{lak_x}{2} \cos\frac{nak_y}{2} \cos\frac{mak_z}{2} \tag{17}$$

($l + n + m = 0, 2, 4, \ldots$, a = 3.603 Å, the sum is over the permutation of the indices x, y, z), the first terms of the series of cubic harmonics[17] $K_i(\theta, \varphi)$, and also combination of the functions (17) and the modulus of the radius vector $(k_x^2 + k_y^2 + k_z^2)^{1/2}$. In both calculations, the number t of terms of the sum (13) did not exceed four. Even at t = 3, and the more so at t = 4, for any of the combinations of test functions given above, the results are accurate within the limit

$$\delta_j = \left| \bar{\nu}_j - T^3 \sum_i a_{ij} w_i \right| \Big/ \bar{\nu}_j \leqslant 10\%.$$

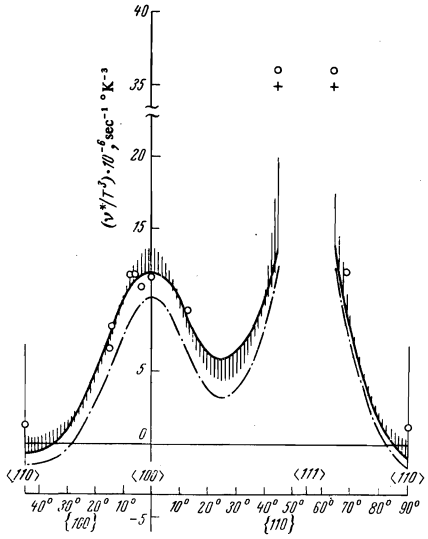

FIG. 4. Anisotropy of the quantity ν^* in the {100} and {110} planes. The shaded bands and the value of ν^* on the neck (denoted by the cross) are the results of our measurements. The points are the measurements of Doezema and Koch. [3] See the text concerning the continuous and dot-dash curves.

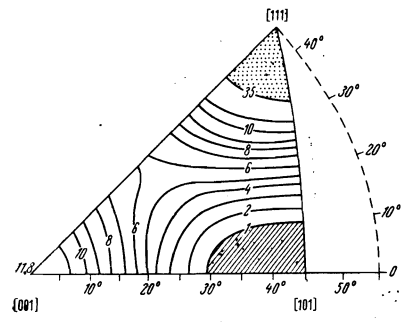

FIG. 5. The function (18) $\nu^*(\mathbf{k})/T^3$ in units of 10^6 sec^{-1} $°K^{-3}$ for the Fermi surface of copper in stereographic projection. There are no reliable data in the shaded regions.

The functions $\nu^*(\mathbf{k})$ were naturally different each time, but the differences were comparatively small. This is seen, for example, from Fig. 4, on the intersections of the function $\nu^*(\mathbf{k})$ with the planes {100} and {110}. The region where the values of the functions $\nu^*(\mathbf{k})$ fall for various functions F_i is shown shaded. The points refer to the results of Doezema and Koch[3], the crosses to the value of ν^* obtained from our experimental result (see the table) from Eq. (12) under the assumption that ν^* and $\nu_\perp$ do not change along the orbit at the neck: $\nu^* = \pi\bar{\nu}_{15}/2$.

In the neighborhood of the ⟨110⟩ direction, the shaded region encloses a region of negative values of ν^*. The fact is that the true value of ν^* in this portion of the Fermi surface is much smaller than the mean value ν^*_{av}. Therefore, the contribution of this region to the integrals (12) and (14) is very small and is comparable with the inaccuracy of the calculations themselves. The inaccuracy of the final results (the bandwidth) is approximately the same over the entire Fermi surface, and was found in this part to be greater than the value of the function itself. Thus, while we have artificially eliminated the region $\nu^*(\mathbf{k}) \gg \nu^*_{av}$ (the vicinity of the neck) from consideration in the first stage of the calculation, the region $\nu^*(\mathbf{k}) \ll \nu^*_{av}$ itself drops out in the course of the calculation.

To be able to estimate the role of the model weighting factor $|\cos\gamma|$ introduced in (12), we have drawn two curves of $\nu^*(\mathbf{k})$ for comparison, both obtained for the same functions F_i. One of them was calculated with account of $|\cos\gamma|$, i.e., with Eq. (12) taken as the starting point; it is described by the formula

$$\nu^*/T^3 = (3{,}16 - 28{,}6F_{110} - 6{,}65F_{200} + 36{,}6F_{211})\cdot 10^6\ \text{sec}^{-1}\,°\text{K}^{-3} \qquad (18)$$

(the solid curve). The second was calculated without $|\cos\gamma|$, starting with formula (10) (the dot-dash curve). It is seen that the weighting factor leads mainly to a shift of the function $\nu^*(\mathbf{k})$ along the ordinate axis, without affecting the location of its extrema on the Fermi surface.

For each of the obtained functions $\nu^*(\mathbf{k})$, we can use Eq. (12) to construct the function $\bar{\nu}(\mathbf{H}/|\mathbf{H}|)$, which in our problem is essentially the initial function (just this function was known at the p points). The result of such calculations for the function (18) at H rotating in the {100} and {110} planes, is shown by the solid curve in Fig. 2. A comparison of this curve with the experimental points 1–13 demonstrates the accuracy of the mathematical algorithm employed. The function (18), constructed over the entire Fermi surface, is shown in Fig. 5. With account of all that has been noted above, this drawing can be regarded as the basic experimental result of our research.

DISCUSSION

First, we should note the coincidence of our results with the results of[5]. From the point of view of the discussion of the correctness of our experiments, this agreement confirms the validity of the choice of the effectiveness weighting factor, introduced in (12). Our first experimental data—the values of ν_j give in Fig. 2 and in the table—agree with the values obtained from the cyclotron-resonance measurements of Häusler and Welles (points 1 and 15). It seems to us that this indicates that even in cyclotron resonance there is an unequal effectiveness of the small-angle scattering along the Larmor orbit. The width of the layer of resonating orbits in cyclotron resonance is determined by the dependence of the cyclotron mass m on k_H. However, another usually smaller dimension of the region of effectiveness, the dimension along the extremal orbit, is more important from the viewpoint of scattering effectiveness. As in the size effect, it is equal to $(\delta/R)k_F$ whereever the electron moves along the normal to the surface of the metal and the scattering leads to a shift in the center of the trajectory along this same direction (R is the Larmor radius). Where the electron moves along the surface and the scattering act involves only its phase or rotation, the dimension of the region of effectiveness is equal to $(\delta/R)^{1/2}k_F$.

Of course, the weighting function $|\cos\gamma|$ is not universal. Measurements of $\bar{\nu}$ on copper at $\mathbf{H} \parallel [100]$ were also performed in[5] by means of ultrasound damping. Here a value of $\bar{\nu}$ was obtained that was half the size of our result and the result of[4]. The same authors assume that the divergence is explained by the fact that the conditions for effectiveness in their experiments were satisfied with an insufficient margin.

Reference was made above to the theoretical calculations of the frequency of electron-phonon collisions in copper, carried out by Nowak[16] by means of a pseudopotential taken from the augmented plane wave model.

Nowak[16] and Doezema and Koch[3] made a comparison of these calculations with experiment and noted their qualitative agreement with the anisotropies of the collision frequency $\nu^*(\mathbf{k})$ experimentally observed in[3], but in the presence of comparatively small quantitative divergences: the experimental points were above the theoretical curve almost everywhere. In relation to the calculation of Nowak[16], there are some obscurities. First, the numerical coefficient $(3/\pi)\zeta(3) \approx 1.15$ obtained by us in Eq. (9), is somewhat different from the coefficient $(24/7\pi)\zeta(3) \approx 1.31$ obtained by Nowak in[16] (see Eq. (9) there), although the course of reasoning is similar. Second, the results of the calculation shown in Figs. 4 and 5 of Nowak's work[16] do not agree with one another. In view of this fact, it seems to us somewhat premature to draw any definitive conclusions as to the significance of the quantitative divergences between theory and experiment.

The authors are grateful to L. G. Fedyaeva and P. D. Mil'man for help and valued advice in the mathematical calculations, to G. I. Kulesko and V. N. Matveev for help in preparation of the samples, to J. Le Hericy for supplying a single crystal of pure copper, and also M. Lee, who kindly sent some preliminary results of his calculations.

[1)]This single crystal was grown by J. Le Hericy (Centre d'etudes de Chimie Metallurgique, France.

[1] M. Springford, Adv. in Phys. 20, 493 (1971).
[2] M. R. Halse, Phil. Trans. Roy. Soc. (London) 265, 507 (1969).
[3] R. E. Doezema and J. F. Koch, Phys. Rev. B6, 2071 (1972).
[4] P. Häusler and S. J. Welles, Phys. Rev. 152, 675 (1966).
[5] M. S. Phua and J. R. Peverly, Phys. Rev. B3, 3115 (1971).
[6] Yu. V. Sharvin and N. I. Bogatina, Zh. Eksp. Teor. Fiz. 56, 772 (1969) [Soviet Phys.-JETP 29, 419 (1969)].
[7] J. Ziman, Electrons and Phonons (Russian translation) IIL, 1962.
[8] V. F. Gantmakher and V. T. Dolgopolov, Zh. Eksp. Teor. Fiz. 60, 2260 (1971) [Soviet Phys.-JETP 33, 1215 (1971)].
[9] V. S. Tsoi and V. F. Gantmakher, Zh. Eksp. Teor. Fiz. 56, 1232 (1969) [Soviet Phys.-JETP 29, 663 (1969)].
[10] E. A. Egorov, Prib. Tekh. Eksp. No. 1, 167 (1963).
[11] V. F. Gantmakher, V. A. Gasparov, G. I. Kulesko, and V. N. Matveev, Zh. Eksp. Teor. Fiz. 63, 1752 (1972) Soviet Phys.-JETP 36, 925 (1973)].
[12] V. L. Naberezhnykh, L. T. Tsymbal, and M. S. Purchinskiĭ, Fiz. Tverd. Tela 14, 518 (1972) [Soviet Phys.-Solid State 14, 431 (1972)].
[13] B. Perrin, G. Weisbuch, and A. Libchaber, Phys. Rev. B1, 1501 (1970).
[14] G. N. Kamm, Phys. Rev. B1, 554 (1970).
[15] J. F. Koch, R. A. Stradling, and A. F. Kip, Phys. Rev. 133, A240 (1964).
[16] D. Nowak, Phys. Rev. B6, 3691 (1972).
[17] M. J. G. Lee and L. N. Falicov, Proc. Roy. Soc. (London) A304, 319 (1968).

Translated by R. T. Beyer
185